Two-Time-Scale Longitudinal Control of Airplanes Using Singular Perturbation

Fu-Chuang Chen* and Hassan K. Khalil†
Michigan State University, East Lansing, Michigan 48824-1226

The singular perturbation approach to the analysis and design of two-time-scale systems is applied to the longitudinal motion of airplanes. Linearized models of longitudinal dynamics have a well known, two-time-scale structure, characterized by the presence of a slow (phugoid) mode and a fast (short-period) mode. Such linearized models are represented in the singularly perturbed form via scaling of state and output variables. The singular perturbation approach is then used to obtain lower-order slow and fast models. The accuracy of these models in approximating eigenvalues is demonstrated using typical numerical data for stable as well as unstable airplanes. The slow and fast models are employed in a sequential design procedure to design a two-time-scale compensator for an unstable transport airplane. In this procedure, a fast compensator is designed first using the fast model; then a slow compensator is designed using a modified slow model. The results of the slow and fast designs are shown to be reasonably recovered when the two-time-scale compensator is applied to the full model.

Nomenclature

c.g. = center of gravity
g_0 = gravity constant, ~32.17 ft/s^2
K_i = integral n_{zu} coefficient, s^{-1}
K_n = ratio of short-term normal acceleration to long-term airspeed change
K_u = proportional speed penalty on velocity
n_z = normal (vertical) acceleration, g
$\overline{n_z}$ = time-scaled normal acceleration, $=\overline{n_z}(p)/\delta_e(p)$
$\overline{N_Z}(p)$ = full normal acceleration transfer function
$\overline{N_{Zf}}(p)$ = fast normal acceleration transfer function
$\overline{N_{Zs}}(s)$ = slow normal acceleration transfer function
n_{zu} = blended normal acceleration and speed
p = high-frequency Laplace operator, $p=j\omega$ on imaginary axis
q = pitch rate, rad/s
s = low-frequency Laplace operator, $=p/\epsilon$
t = slow time scale, $=\epsilon\tau$
v = incremental forward velocity, ft/s
$\bar{v}$ = time-scaled incremental forward velocity, $=(\epsilon/V_0)v$
$\overline{V}(p)$ = full incremental forward velocity transfer function, $=\bar{v}(p)/\delta_e(p)$
$\overline{V}_f(p)$ = fast incremental forward velocity transfer function
$\overline{V}_s(s)$ = slow incremental forward velocity transfer function
V_0 = forward velocity, ft/s
α = angle of attack, rad
δ_e = elevator position, rad
δ_{ec} = elevator command, rad
δ_{servo} = servo position, rad
ϵ = a small positive number representing the separation of fast and slow dynamics
ζ = damping ratio
θ = pitch angle, rad
$\bar{\theta}$ = time-scaled pitch angle, $=\epsilon\theta$
λ = eigenvalue
τ = fast time scale, s
ω = frequency, rad/s
ω_n = natural frequency, rad/s

Received Feb. 5, 1988; presented as Paper 88-4112 at the AIAA Guidance, Navigation, and Control Conference, Minneapolis, MN, Aug. 15-17, 1988; revision received May 29, 1989.

*Graduate Student, Department of Electrical Engineering.
†Professor, Department of Electrical Engineering.

I. Introduction

CLASSICAL designs of longitudinal feedback control[1,2] are based on clear exploitation of the multiple-time-scale structure of the system. They reveal a very interesting and intuitive way of separating the design goals into slow and fast ones and using separate approximate models to design feedback controls that achieve the control goals. An example of this is the phugoid supression feedback control of Ref. 1 that uses feedback from the pitch angle θ and an approximate transfer function of the phugoid motion to design feedback that supresses the lightly damped, low-frequency oscillation associated with the phugoid motion. Another example is the longitudinal approach control system of Chap. 11 of Ref. 2, where the design of the controller is based on separate low-frequency and high-frequency considerations. Despite this interesting role of the time-scale structure in classical design, the idea is not exploited in the many applications of modern control methods to design longitudinal autopilot, e.g., Refs. 3-6.

The decomposition of a full model into lower-order slow and fast models, and the exploitation of this decomposition in analysis and design, is the main theme of the singular perturbation approach to the control of multiple-time-scale systems.[7,8] In this paper the singular perturbation method is applied to the longitudinal control problem. The method is used to derive slow and fast models that represent the phugoid and short-period modes, respectively. These models are then used to synthesize a feedback control law.

In Sec. II, a few results from singular perturbation theory are reviewed, and the sequential design procedure of Ref. 9 for synthesizing a two-time-scale stabilizing compensator is outlined. In Sec. III, a procedure is introduced to model the longitudinal dynamics of an airplane into the singularly perturbed form. Slow and fast models are then derived, and their accuracy in approximating the eigenvalues is demonstrated by

numerical examples. In Sec. IV, a design example is worked out to demonstrate the sequential design procedure of Ref. 9.

II. Singularly Perturbed Systems and the Sequential Design Methodology

A singularly perturbed, linear, time-invariant system is represented by[3]

$$\frac{dx}{d\tau} = \epsilon A_{11}(\epsilon)x + \epsilon A_{12}(\epsilon)z + \epsilon B_1(\epsilon)u \tag{1}$$

$$\frac{dx}{d\tau} = A_{21}(\epsilon)x + A_{22}(\epsilon)z + B_2(\epsilon)u, \quad \det\left[A_{22}(0)\right] \neq 0 \tag{2}$$

$$y = C_1(\epsilon)x + C_2(\epsilon)z + E(\epsilon)u \tag{3}$$

where $x \in R^n$ comprises the slow state variables, $z \in R^m$ comprises the fast state variables, $u \in R^p$ is the control input, and $y \in R^q$ is the output. The small positive constant ϵ represents the separation of the slow and the fast dynamics in the sense that $dx/d\tau$ is $\mathcal{O}(\epsilon)$ [a function $f(\epsilon)$ is said to be $\mathcal{O}(\epsilon^\gamma)$, for $\gamma \geq 0$, if $|f(\epsilon)| \leq K\epsilon^\gamma$, for $\epsilon < \epsilon^*$, where K is a positive constant independent of ϵ], whereas $dz/d\tau$ is $\mathcal{O}(1)$. In the singular perturbation literature (e.g., Ref. 7), it is more common to represent the system in a slow time scale $t = \epsilon\tau$. But, in this paper, the fast time scale τ will be used since the airplane longitudinal dynamics will be modeled in the form of Eqs. (1-3).

For small ϵ, the singularly perturbed system of Eqs. (1-3) has a two-time-scale structure, where the eigenvalues cluster into a group of slow eigenvalues of order $\mathcal{O}(\epsilon)$ and a group of fast eigenvalues of order $\mathcal{O}(1)$. This two-time-scale structure can be seen through a similarity transformation that decouples the slow and fast dynamics. It is shown in Ref. 7 that there exist matrices $L(\epsilon)$ and $H(\epsilon)$, analytic in ϵ at $\epsilon = 0$, such that the similarity transformation

$$\begin{bmatrix} x \\ z \end{bmatrix} = \begin{bmatrix} I_n & \epsilon H(\epsilon) \\ -L(\epsilon) & I_m - \epsilon L(\epsilon)H(\epsilon) \end{bmatrix} \begin{bmatrix} \zeta \\ \eta \end{bmatrix} \tag{4}$$

transforms the system of Eqs. (1-3) into the decoupled form

$$\begin{bmatrix} \frac{d\zeta}{d\tau} \\ \frac{d\eta}{d\tau} \end{bmatrix} = \begin{bmatrix} \epsilon A_s(\epsilon) & 0 \\ 0 & A_f(\epsilon) \end{bmatrix} \begin{bmatrix} \zeta \\ \eta \end{bmatrix} + \begin{bmatrix} \epsilon B_s(\epsilon) \\ B_f(\epsilon) \end{bmatrix} u \tag{5}$$

$$y = \begin{bmatrix} C_s(\epsilon) & C_f(\epsilon) \end{bmatrix} \begin{bmatrix} \zeta \\ \eta \end{bmatrix} + Eu \tag{6}$$

where

$$\begin{aligned} A_s &= A_{11} - A_{12}L, & B_s &= B_1 - HB_2 - \epsilon HLB_1 \\ A_f &= A_{22} + \epsilon LB_1, & B_f &= B_2 + \epsilon LB_1 \\ C_s &= C_1 - C_2L, & C_f &= C_2 + \epsilon(C_1 - C_2L)H \end{aligned} \tag{7}$$

and L and H satisfy the equations

$$A_{21} - A_{22}L + \epsilon LA_{11} - \epsilon LA_{12}L = 0 \tag{8}$$

$$\epsilon(A_{11} - A_{12}L)H - H(A_{22} + \epsilon LA_{12}) + A_{12} = 0 \tag{9}$$

The transformation (4) can be viewed as a block modal decomposition where the columns of $[I_n \quad -L']'$ span the invariant subspace associated with the slow eigenvalues, and the columns of $[\epsilon H' \quad I_m - \epsilon H'L']'$ span the invariant subspace associated with the fast eigenvalues. The two-time-scale structure of the system is clear from the block modal form of Eq. (5). The fact that the block ϵH in Eq. (4) is $\mathcal{O}(\epsilon)$ shows that the contribution of the fast modes in x is only $\mathcal{O}(\epsilon)$, which justifies calling x the slow variables. Inspection of Eqs. (8) and (9) shows that

$$L = A_{22}^{-1}A_{21} + \mathcal{O}(\epsilon), \qquad H = A_{12}A_{22}^{-1} + \mathcal{O}(\epsilon) \tag{10}$$

Substitution of Eq. (10) into Eq. (7) yields

$$\begin{aligned} A_s &= A_{11} - A_{12}A_{22}^{-1}A_{21} + \mathcal{O}(\epsilon), & B_s &= B_1 - A_{12}A_{22}^{-1}B_2 + \mathcal{O}(\epsilon) \\ A_f &= A_{22} + \mathcal{O}(\epsilon), & B_f &= B_2 + \mathcal{O}(\epsilon) \\ C_s &= C_1 - C_2A_{22}^{-1}A_{21} + \mathcal{O}(\epsilon), & C_f &= C_2 + \mathcal{O}(\epsilon) \end{aligned} \tag{11}$$

Hence the decoupled subsystems of Eqs. (5) and (6) can be approximated by the slow and fast models.

Slow model:

$$\frac{dx_s}{dt} = (A_0x_s + B_0u), \qquad t = \epsilon\tau \tag{12}$$

$$y_s = C_0x_s + E_0u \tag{13}$$

where $A_0 = A_{11} - A_{12}A_{22}^{-1}A_{21}$, $B_0 = B_1 - A_{12}A_{22}^{-1}B_2$, $C_0 = C_1 - C_2A_{22}^{-1}A_{21}$, and $E_0 = E - C_2A_{22}^{-1}B_2$.

Fast model:

$$\frac{dz_f}{d\tau} = A_{22}z_f + B_2u \tag{14}$$

$$y_f = C_2z_f + Eu \tag{15}$$

The coefficient of the feed-through term $(E - C_2A_{22}^{-1}B_2)$ of the slow model is the *DC* (or steady-state) gain of the fast model. These same slow and fast models can be obtained directly from the full model [Eqs. (1-3)] via intuitive arguments. The slow model [Eqs. (12) and (13)] is obtained by assuming that the fast motion has reached a quasi-steady-state where Eq. (2) can be replaced by an algebraic equation, which is then used to eliminate z from Eqs. (1) and (3). The fast model is obtained by assuming that, during the fast motion, x is a constant bias in Eqs. (2) and (3). Eliminating this bias leads to the fast model of Eqs. (14) and (15).

Various properties of the singularly perturbed model of Eqs. (1-3) can be approximated for sufficiently small ϵ by the corresponding properties of the slow and fast models of Eqs. (12-15). Two approximations that are used in this paper are eigenvalue and transfer function approximations.

Eigenvalue Approximation

As $\epsilon \to 0$, the slow eigenvalues of the full singularly perturbed model of Eqs. (1-3) approach $\epsilon\lambda_i's$, where $\lambda_i's$ are the eivenvalues of the slow model of Eqs. (12) and (13); the fast eigenvalues of Eqs. (1-3) approach the eigenvalues of the fast model of Eqs. (14) and (15). This statement, which follows from continuous dependence of the eigenvalues of a matrix on its parameters, is proved in Ref. 7. Furthermore, if all the eigenvalues of the slow and fast modes are distinct, the approximation errors will be $\mathcal{O}(\epsilon^2)$ in the case of the slow eigenvalues and $\mathcal{O}(\epsilon)$ in the case of the fast eigenvalues.

Transfer Function Approximation

Let $G(p,\epsilon)$ be the transfer function of the full singularly perturbed model of Eqs. (1-3). Let $G_s(s)$ and $G_f(p)$ be the transfer functions of the slow and fast models, respectively, i.e.,

$$G_s(s) = C_0(sI - A_0)^{-1}B_0 + E_0 \tag{16}$$

$$G_f(p) = C_2(pI - A_{22})^{-1}B_2 + E \tag{17}$$

Here $s=p/\epsilon$ is the low frequency scale. Note that

$$G_s(\infty) = G_f(0) \tag{18}$$

and $G_f(p)$ has no poles at the origin since A_{22} is nonsingular. It is shown in Ref. 10 that

$$G(p,\epsilon) = G_s(s) + G_f(p) - G_s(\infty) + \mathcal{O}(\epsilon) \tag{19}$$

on the imaginary axis $p=j\omega$.

Output feedback control of singularly perturbed systems is studied in Ref. 9 using recent results on parameterization of stabilizing compensators, e.g., Ref. 11. The results of Ref. 9 parameterize all singularly perturbed compensators that can stabilize a singularly perturbed plant while preserving its two-time-scale structure. These results are then used to devise the following sequential design procedure.

First

A fast compensator $C_f(p)$ is designed to stabilize the high-frequncy closed-loop $[C_f(p), G_f(p)]$ and to meet high-frequency design objectives. The compensator $C_f(p)$ cannot have poles at the origin.

Second

A slow compensator $C_s(s)$ is designed, subject to the constraint

$$C_s(\infty) = C_f(0) \tag{20}$$

to stabilize the low-frequency closed-loop $[C_s(s), G_s(s)]$ and to meet other low-frequency design objectives. It is shown in Ref. 9 that the strictly proper part $C_0(s)=C_s(s)-C_f(0)$ of $C_s(s)$ stabilizes a modified slow model

$$\hat{G}_s(s) = G_s(s)\left[I + G_f(0)G_s(s)\right]^{-1} \tag{21}$$

Third

A compensator $C(p,\epsilon)$ is taken as the parallel connection

$$C(p,\epsilon) = C_0(p/\epsilon) + C_f(p) \tag{22}$$

It is shown in Ref. 9 that the closed-loop system $[C(p,\epsilon), G(p,\epsilon)]$ will be asymptotically stable for sufficiently small ϵ. Moreover, any point-to-point transfer function in $[C(p,\epsilon), G(p,\epsilon)]$ can be approximated by the corresponding slow and fast transfer functions, as in Eq. (19).

The preceding sequential procedure decomposes the design problem into two lower-order design problems. Design compromises for low-frequency and high-frequency bands are achieved separately. Design calculations are performed on the slow and fast models, thus alleviating high dimensionality and ill conditioning associated with the full singularly perturbed model. The parallel connection of Eq. (22) can be realized using separate networks in different time scales. In the case of digital implementation, different sampling rates can be used for the two parts since the strictly proper slow compensator $C_0(s)$ will have a bandwidth much narrower than the bandwidth of the fast compensator $C_f(p)$.

III. Modeling Longitudinal Dynamics in the Singularly Perturbed Form

A slow "phugoid mode" and a fast "short-period mode" are well-known time-scale characteristics of the longitudinal motion of an airplane. A linearized longitudinal model for the straight steady flight with forward velocity V_0 (ft/s) is given by Ref. 1:

$$\frac{\mathrm{d}}{\mathrm{d}\tau}\begin{bmatrix} v \\ \theta \\ \alpha \\ q \end{bmatrix} = \begin{bmatrix} X_v & -g_0 & X_\alpha & 0 \\ 0 & 0 & 0 & 1 \\ Z_v & 0 & Z_\alpha & 1 \\ M_v & 0 & M_\alpha & M_q \end{bmatrix}\begin{bmatrix} v \\ \theta \\ \alpha \\ q \end{bmatrix} + \begin{bmatrix} X_\delta \\ 0 \\ Z_\delta \\ M_\delta \end{bmatrix}\delta_e \tag{23}$$

$$\begin{bmatrix} n_z \\ v \end{bmatrix} = \begin{bmatrix} \dfrac{x_a M_v - V_0 Z_v}{g_0} & 0 & \dfrac{x_a M_\alpha - V_0 Z_\alpha}{g_0} & \dfrac{x_a M_q}{g_0} \\ 1 & 0 & 0 & 0 \end{bmatrix}\begin{bmatrix} v \\ \theta \\ \alpha \\ q \end{bmatrix} + \begin{bmatrix} \dfrac{x_a M_\delta - V_0 Z_\delta}{g_0} \\ 0 \end{bmatrix}\delta_e \tag{24}$$

where v, θ, α, q, and δ_e are, respectively, incremental forward velocity (ft/s), pitch angle (rad), angle of attack (rad), pitch rate (rad/s), and elevator position (rad); n_z is normal acceleration (g), which is measured at some distance, x_a (ft), from the center of gravity (x_a is forward positive). The time τ in Eq. (23) is measured in seconds. In addition to n_z and v, there are other output variables of control interest, e.g., θ, α, and q. Since only n_z and v will be used for output feedback design in Sec. IV, other variables are omitted from the output of Eq. (24).

To apply singular perturbation theory, a singularly perturbed model of the longitudinal dynamics is needed. First, a small positive parameter ϵ has to be chosen to represent the separation of fast and slow dynamics. The parameter ϵ is taken as the ratio of the largest of the phugoid mode eivenvalues to the smallest of the short-period mode eivenvalues. Second, the state equation should be brought into a form where the A and B matrices can be partitioned as

$$A = \begin{bmatrix} \epsilon F_{11} & \epsilon F_{12} \\ F_{21} & F_{22} \end{bmatrix}, \qquad B = \begin{bmatrix} \epsilon G_1 \\ G_2 \end{bmatrix} \tag{25}$$

where the partition is compatible with the number of slow and fast eigenvalues, and F_{22} is nonsingular. Naturally, it is preferable to do this while preserving the given physical state variables. For the longitudinal state equation (23), it is well known that α and q are candidates to be considered fast variables. This leaves v and θ as candidates to be slow variables. Partitioning Eq. (23) accordingly, it can be seen that, for typical numerical data, the matrix F_{22} is indeed nonsingular. However, the matrices of the first block row are not $\mathcal{O}(\epsilon)$ as required in Eq. (25). For example, the element $-g_0$ has a magnitude 32.2, which clearly is not $\mathcal{O}(\epsilon)$. This particular element can be scaled down by scaling the velocity. Therefore, it was decided to replace v by v/V_0 as a state variable. With this scaling it was found that, for typical numerical data, the matrices A and B of the longitudinal state equation take the form

$$A = \begin{bmatrix} \epsilon F_{11} & F_{12} \\ \epsilon F_{21} & F_{22} \end{bmatrix}, \qquad B = \begin{bmatrix} \epsilon G_1 \\ G_2 \end{bmatrix} \tag{26}$$

The form of the matrix A in Eq. (26) is dual to the form of the matrix A in Eq. (25) in the sense that A^T in Eq. (26) takes the form of A in Eq. (25). It is shown in Ref. 7 that the matrix A in Eq. (26) can be brought into the singularly perturbed form of Eq. (25) either by a similarity transformation

$$\begin{bmatrix} I & -F_{12}F_{22}^{-1} \\ 0 & I \end{bmatrix} \tag{27}$$

or by scaling

$$\begin{bmatrix} \epsilon I & 0 \\ 0 & I \end{bmatrix} \tag{28}$$

It can be easily verified that

$$\begin{bmatrix} I & -F_{12}F_{22}^{-1} \\ 0 & I \end{bmatrix}\begin{bmatrix} \epsilon F_{11} & F_{12} \\ \epsilon F_{21} & F_{22} \end{bmatrix}\begin{bmatrix} I & F_{12}F_{22}^{-1} \\ 0 & I \end{bmatrix} = \begin{bmatrix} \epsilon\tilde{F}_{11} & \epsilon F_{12} \\ \epsilon\tilde{F}_{21} & \tilde{F}_{22} \end{bmatrix} \tag{29}$$

and

$$\begin{bmatrix} \epsilon I & 0 \\ 0 & I \end{bmatrix}\begin{bmatrix} \epsilon F_{11} & F_{12} \\ \epsilon F_{21} & F_{22} \end{bmatrix}\begin{bmatrix} \frac{1}{\epsilon}I & 0 \\ 0 & I \end{bmatrix} = \begin{bmatrix} \epsilon F_{11} & \epsilon F_{12} \\ F_{21} & F_{22} \end{bmatrix} \tag{30}$$

Notice that $\epsilon\tilde{F}_{21}$ can be viewed as an $\mathcal{O}(1)$ quantity since it is bounded by a constant independent of ϵ for sufficiently small ϵ. Thus, for homogeneous motion, either one of the two transformations of Eqs. (27) and (28) can be used. However, only Eq. (28) can bring the matrix B of Eq. (26) into the form of the matrix B of Eq. (25). Therefore, it was decided to use the scaling similarity transformation of Eq. (28). The scaled state variables are

$$\bar{v} = \frac{\epsilon}{V_0}v \tag{31}$$

$$\bar{\theta} = \epsilon\theta \tag{32}$$

Since the output matrices in the singularly perturbed form of Eq. (24) should be $\mathcal{O}(1)$, the output variable n_z is scaled as well:

$$\bar{n}_z = \frac{g_0}{V_0}n_z \tag{33}$$

With the scaling of Eqs. (31-33), the longitudinal model is rewritten as

$$\frac{\mathrm{d}}{\mathrm{d}\tau}\begin{bmatrix} \bar{v} \\ \bar{\theta} \\ \alpha \\ q \end{bmatrix} = \begin{bmatrix} X_v & \frac{-g_0}{V_0} & \frac{X_\alpha\epsilon}{V_0} & 0 \\ 0 & 0 & 0 & \epsilon \\ \frac{Z_vV_0}{\epsilon} & 0 & Z_\alpha & 1 \\ \frac{M_vV_0}{\epsilon} & 0 & M_\alpha & M_q \end{bmatrix}\begin{bmatrix} \bar{v} \\ \bar{\theta} \\ \alpha \\ q \end{bmatrix} + \begin{bmatrix} \frac{X_\delta\epsilon}{V_0} \\ 0 \\ Z_\delta \\ M_\delta \end{bmatrix}\delta_e \tag{34}$$

$$\begin{bmatrix} \bar{n}_z \\ \bar{v} \end{bmatrix} = \begin{bmatrix} \frac{x_aM_v - V_0Z_v}{\epsilon} & 0 & \frac{x_aM_\alpha - V_0Z_\alpha}{V_0} & \frac{x_aM_q}{V_0} \\ 1 & 0 & 0 & 0 \end{bmatrix}\begin{bmatrix} \bar{v} \\ \bar{\theta} \\ \alpha \\ q \end{bmatrix} + \begin{bmatrix} \frac{x_aM_\delta - V_0Z_\delta}{V_0} \\ 0 \end{bmatrix}\delta_e \tag{35}$$

For typical numerical values, the quantities

$$X_v,\ \frac{-g_0}{V_0},\ \frac{X_\alpha\epsilon}{V_0},\ \frac{X_\delta\epsilon}{V_0} \text{ are } \mathcal{O}(\epsilon)$$

whereas

$$\frac{Z_vV_0}{\epsilon},\ Z_\alpha,\ Z_\delta,\ \frac{M_vV_0}{\epsilon},\ M_\alpha,\ M_q,\ M_\delta,\ \frac{x_aM_v - V_0Z_v}{\epsilon}$$

$$\frac{x_aM_\alpha - V_0Z_\alpha}{V_0},\ \frac{x_aM_q}{V_0},\ \text{and}\ \frac{x_aM_\delta - V_0Z_\delta}{V_0} \text{ are } \mathcal{O}(1)$$

Therefore, the model of Eqs. (34) and (35) is in the singularly perturbed form of Eqs. (1-3) with α and q as the fast variables and $\bar{v}$ and $\bar{\theta}$ as the slow variables. Then, the slow and fast models are given as follows.

Slow model:

$$\frac{\mathrm{d}}{\mathrm{d}\tau}\begin{bmatrix} \bar{v} \\ \bar{\theta} \end{bmatrix} = \begin{bmatrix} \hat{A}_{11} & \frac{-g_0}{V_0} \\ \hat{A}_{21} & 0 \end{bmatrix}\begin{bmatrix} \bar{v} \\ \bar{\theta} \end{bmatrix} + \begin{bmatrix} \hat{B}_1 \\ \hat{B}_2 \end{bmatrix}\delta_e \tag{36}$$

$$\begin{bmatrix} \bar{n}_z \\ \bar{v} \end{bmatrix} = \begin{bmatrix} \hat{C}_{11} & 0 \\ 1 & 0 \end{bmatrix}\begin{bmatrix} \bar{v} \\ \bar{\theta} \end{bmatrix} + \begin{bmatrix} \hat{E}_1 \\ 0 \end{bmatrix}\delta_e \tag{37}$$

where

$$\hat{A}_{11} = X_v - \frac{X_\alpha(M_qZ_v - M_v)}{Z_\alpha M_q - M_\alpha},\quad \hat{A}_{21} = \frac{-V_0(Z_\alpha M_v - Z_vM_\alpha)}{Z_\alpha M_q - M_\alpha}$$

$$\hat{B}_1 = \frac{\epsilon X_\delta}{V_0} - \frac{\epsilon X_\alpha(M_qZ_\delta - M_\delta)}{V_0(Z_\alpha M_q - M_\alpha)},\quad \hat{B}_2 = \frac{\epsilon(M_\alpha Z_\delta - M_\delta Z_\alpha)}{Z_\alpha M_q - M_\alpha}$$

$$\hat{C}_{11} = \frac{x_aM_v - V_0Z_\alpha}{\epsilon} - \frac{(x_aM_\alpha - V_0Z_\alpha)(M_qZ_v - M_v)}{\epsilon(Z_\alpha M_q - M_\alpha)} - \frac{x_aM_q(Z_\alpha M_v - M_\alpha Z_v)}{\epsilon(Z_\alpha M_q - M_\alpha)}$$

$$\hat{E}_1 = \frac{x_aM_\delta - V_0Z_\delta}{V_0} - \frac{(x_aM_q - V_0Z_\alpha)(M_qZ_\delta - M_\delta)}{V_0(Z_\alpha M_q - M_\alpha)} - \frac{x_aM_q(Z_\alpha M_\delta - M_\alpha Z_\delta)}{V_0(Z_\alpha M_q - M_\alpha)}$$

Fast model:

$$\frac{\mathrm{d}}{\mathrm{d}\tau}\begin{bmatrix} \alpha \\ q \end{bmatrix} = \begin{bmatrix} Z_\alpha & 1 \\ M_\alpha & M_q \end{bmatrix}\begin{bmatrix} \alpha \\ q \end{bmatrix} + \begin{bmatrix} Z_\delta \\ M_\delta \end{bmatrix}\delta_e \tag{38}$$

$$\begin{bmatrix} \bar{n}_z \\ \bar{v} \end{bmatrix} = \begin{bmatrix} \frac{x_aM_\alpha - V_0Z_\alpha}{V_0} & \frac{x_aM_q}{V_0} \\ 0 & 0 \end{bmatrix}\begin{bmatrix} \alpha \\ q \end{bmatrix} + \begin{bmatrix} \frac{x_aM_\delta - V_0Z_\delta}{V_0} \\ 0 \end{bmatrix}\delta_e \tag{39}$$

To appreciate the value of the singular perturbation decomposition, let us use the slow and fast models [Eqs. (36) and (38)] to approximate the eigenvalues of the open-loop system and to compare such approximations with the standard approximations in the flight dynamics literature, e.g., Refs. 1 and 2. From the fast model of Eq. (38), the eigenvalues of the short-period mode are approximated by the roots of the equation

$$p^2 - (Z_\alpha + M_q)p + Z_\alpha M_q - M_\alpha = 0 \tag{40}$$

From the slow model of Eq. (36), the eigenvalues of the phugoid mode are approximated by the roots of the equation

$$p^2 + \left[-X_v + \frac{X_\alpha(Z_vM_q - M_v)}{Z_\alpha M_q - M_\alpha}\right]p + \frac{g_0(M_\alpha Z_v - M_vZ_\alpha)}{Z_\alpha M_q - M_\alpha} = 0 \tag{41}$$

The short-period approximation (40) agrees with a standard approximation that can be found in the flight dynamics literature, e.g., Refs. 1 and 2. The phugoid approximation (41) is different from the standard approximations reported in Refs. 1 and 2. In Ref. 2, a so-called three-degree-of-freedom phugoid approximation is obtained by replacing the pitching moment equation of Eq. (23), i.e., $\mathrm{d}q/\mathrm{d}\tau = M_vv + M_\alpha\alpha + M_qq$

$+M_\delta\delta_e$ by the algebraic equation

$$0 = M_v v + M_\alpha \alpha + M_\delta \delta_e \tag{42}$$

This leads to

$$p^2 + \left[-X_v + \frac{(X_\alpha - g_0)M_v}{M_\alpha} \right] p - \frac{g_0(Z_v M_\alpha - Z_\alpha M_v)}{M_\alpha} = 0 \tag{43}$$

Moreover, neglecting M_v yields the so-called two-degree-of-freedom approximation given by

$$p^2 - X_v p - Z_v g_0 = 0 \tag{44}$$

which is the same phugoid approximation reported in Ref. 1. It is interesting to notice that Eq. (44) follows from the singular perturbation approximation of Eq. (41) when the following additional assumptions hold:

$$Z_\alpha M_q - M_\alpha \sim -M_\alpha \tag{45}$$

$$M_\alpha Z_v - M_v Z_\alpha \sim M_\alpha Z_v \tag{46}$$

$$|(Z_v M_q - M_v)X_\alpha| \ll |(Z_\alpha M_q - M_\alpha)X_v| \tag{47}$$

These three assumptions will typically hold when M_α is negative and large in magnitude, i.e., for stable airplanes. The three approximations [Eqs. (41), (43), and (44)] are illustrated using typical numerical data from Refs. 4 and 12. The F-8 airplane of Ref. 4 has the following data:

$$X_v = -0.015, \qquad g = 32.2, \qquad X_\alpha = -14.1$$

$$Z_v = -0.00019, \qquad Z_\alpha = -0.84$$

$$M_v = 0.00005, \qquad M_\alpha = -4.8, \qquad M_q = -0.049$$

The exact phugoid mode eigenvalues as well as the approximate eigenvalues determined by the three-degree-of-freedom (3DOF) approximation of Eq. (43), the two-degree-of-freedom (2DOF) approximation of Eq. (44), and the singular perturbation (SPT) approximation of Eq. (41) are shown in the following:

Exact: $-0.0069 \pm j0.0765$

3DOF: $-0.0077 \pm j0.0796$

2DOF: $-0.0075 \pm j0.0779$

SPT: $-0.0074 \pm j0.0764$

The results show that the SPT approximation is slightly better than the standard ones, although all three approximations are quite adequate. This is typical for stable airplanes for which M_α is negative and its magnitude is large enough to justify the approximation of Eqs. (45) and (46). Consider, next, the numerical data of the unstable airplane of Ref. 12:

$$X_v = -0.01365, \qquad g = 32.2, \qquad X_\alpha = 10.19$$

$$Z_v = -0.00026, \qquad Z_\alpha = -0.752$$

$$M_v = 0.0000186, \qquad M_\alpha = 0.079, \qquad M_q = -0.8725$$

The exact and approximate eigenvalues of the phugoid mode are given by

Exact: $0.012, -0.0318$

3DOF: $-0.0042 \pm j0.0897$

2DOF: $-0.0068 \pm j0.09198$

SPT: $0.0128, -0.030$

In this case only the singular perturbation approximation is acceptable. While standard approximations fail even to predict the instability of the phugoid motion, the singular perturbation method can still provide a good approximation. This is explained by the fact stated in Sec. II that eigenvalues of the slow model are $\mathcal{O}(\epsilon^2)$ close to the slow eigenvalues of the full model.

IV. Two-Time-Scale Longitudinal Autopilot Design

In this section the sequential design procedure described in Sec. II is used to synthesize a two-time-scale longitudinal autopilot for an unstable transport airplane. More information about flight conditions and open-loop characteristics of this airplane can be found in Ref. 12 or case II of Ref. 3. The linear model of the longitudinal dynamics of this airplane under CRUISE condition with center of gravity at 50% mean aerodynamic chord (MAC) and forward velocity $V_0 = 778$ ft/s is given by

$$\frac{d}{d\tau}\begin{bmatrix} v \\ \theta \\ \alpha \\ q \end{bmatrix} = \begin{bmatrix} -0.01365 & -32.2 & 10.19 & 0 \\ 0 & 0 & 0 & 1 \\ -0.00026 & 0 & -0.752 & 0 \\ 0.0000186 & 0 & 0.079 & -0.8725 \end{bmatrix} \times \begin{bmatrix} v \\ \theta \\ \alpha \\ q \end{bmatrix} + \begin{bmatrix} 2.135 \\ 0 \\ -0.06311 \\ -3.399 \end{bmatrix} \delta_e \tag{48}$$

$$\begin{bmatrix} n_z \\ v \end{bmatrix} = \begin{bmatrix} 0.00646 & 0 & 18.20 & -0.401 \\ 1.0 & 0 & 0 & 0 \end{bmatrix} \begin{bmatrix} v \\ \theta \\ \alpha \\ q \end{bmatrix} + \begin{bmatrix} 0.047 \\ 0 \end{bmatrix} \delta_e \tag{49}$$

where normal acceleration n_z is measured at a location 14.0 ft forward of c.g., resulting in two zeros 32.3 rad/s and -38 rad/s on the real axis outside the expected control-loop bandwidth. (The equation of n_z is extrapolated from the data given in Ref. 12 for the given choice of x_a. All other equations are taken exactly from Ref. 12.) The linear model of the actuator dynamics is given by

$$\frac{d}{d\tau}\begin{bmatrix} \delta_e \\ \delta_{\text{servo}} \end{bmatrix} = \begin{bmatrix} -20 & 10.72 \\ 0 & -50 \end{bmatrix} \begin{bmatrix} \delta_e \\ \delta_{\text{servo}} \end{bmatrix} + \begin{bmatrix} 0 \\ 50 \end{bmatrix} \delta_{ec} \tag{50}$$

$$\delta_e = \begin{bmatrix} 1 & 0 \end{bmatrix} \begin{bmatrix} \delta_e \\ \delta_{\text{servo}} \end{bmatrix} \tag{51}$$

The eigenvalues of the open-loop system are given by

$$\left.\begin{aligned} \lambda_1 &= 0.012 \\ \lambda_2 &= -0.0318 \end{aligned}\right\} \quad \text{unstable phugoid mode}$$

$$\left.\begin{aligned} \lambda_3 &= -0.519 \\ \lambda_2 &= -1.1 \end{aligned}\right\} \quad \text{short-period mode}$$

$$\left.\begin{aligned} \lambda_5 &= -20.0 \\ \lambda_2 &= -50.0 \end{aligned}\right\} \quad \text{actuator}$$

Before proceeding to the two-time-scale design, airplane longitudinal dynamics in Eqs. (48) and (49) have to be transformed into singularly perturbed form. By setting ϵ to be the

ratio of the largest phugoid eigenvalue to the smallest short-period eigenvalue, i.e., $\epsilon = 0.0318/0.519 = 0.0613$, and carrying out the state and output scaling,

$$\bar{v} = \frac{\epsilon}{V_0} v = 0.0000788 v$$

$$\bar{\theta} = \epsilon\theta = 0.0613\theta$$

$$\overline{n_z} = \frac{g_0}{V_0} n_z = 0.0415 n_z$$

on Eqs. (48) and (49), the following singularly perturbed model is obtained:

Full model:

$$\frac{d}{d\tau}\begin{bmatrix}\bar{v}\\ \bar{\theta}\\ \alpha\\ q\end{bmatrix} = \begin{bmatrix}-0.01365 & -0.04132 & 0.000804 & 0\\ 0 & 0 & 0 & 0.0613\\ -3.358 & 0.0207 & -0.752 & 1.001\\ 0.237 & 0 & 0.079 & -0.8725\end{bmatrix} \times \begin{bmatrix}\bar{v}\\ \bar{\theta}\\ \alpha\\ q\end{bmatrix} + \begin{bmatrix}-0.000168\\ 0\\ -0.06311\\ -3.399\end{bmatrix}\delta_e \tag{52}$$

$$\begin{bmatrix}\overline{n_z}\\ \bar{v}\end{bmatrix} = \begin{bmatrix}3.362 & -0.0207 & 0.753 & -0.0167\\ 1.0 & 0 & 0 & 0\end{bmatrix}\begin{bmatrix}\bar{v}\\ \bar{\theta}\\ \alpha\\ q\end{bmatrix} + \begin{bmatrix}0.001946\\ 0\end{bmatrix}\delta_e \tag{53}$$

The slow and fast models are given by

Slow model:

$$\frac{d}{d\tau}\begin{bmatrix}\bar{v}\\ \bar{\theta}\end{bmatrix} = \begin{bmatrix}-0.2838 & -0.6736\\ -0.151 & 0.002835\end{bmatrix}\begin{bmatrix}\bar{v}\\ \bar{\theta}\end{bmatrix} + \begin{bmatrix}-0.0813\\ -4.438\end{bmatrix}\delta_e \tag{54}$$

$$\begin{bmatrix}\overline{n_z}\\ \bar{v}\end{bmatrix} = \begin{bmatrix}-0.151 & 0.002834\\ 1.0 & 0\end{bmatrix}\begin{bmatrix}\bar{v}\\ \bar{\theta}\end{bmatrix} + \begin{bmatrix}-4.438\\ 0\end{bmatrix}\delta_e \tag{55}$$

where $t = \epsilon\tau$.

Fast model:

$$\frac{d}{d\tau}\begin{bmatrix}\alpha\\ q\end{bmatrix} = \begin{bmatrix}-0.752 & 1.001\\ 0.079 & -0.8725\end{bmatrix}\begin{bmatrix}\alpha\\ q\end{bmatrix} + \begin{bmatrix}-0.06311\\ -3.399\end{bmatrix}\delta_e \tag{56}$$

$$\begin{bmatrix}\overline{n_z}\\ \bar{v}\end{bmatrix} = \begin{bmatrix}0.753 & -0.0167\\ 0 & 0\end{bmatrix}\begin{bmatrix}\alpha\\ q\end{bmatrix} + \begin{bmatrix}0.001946\\ 0\end{bmatrix}\delta_e \tag{57}$$

The transfer functions of the full, slow, and fast models are given by the following equations.

Full transfer functions:

$$\overline{N_Z}(p) = \frac{\overline{n_z}(p)}{\delta_e(p)} = \frac{0.001945(p-33.49)(p+39.57)(p+0.005864)(p+0.000002911)}{(p+0.519)(p+1.1)(p+0.0318)(p-0.0122)} \tag{58}$$

$$\bar{V}(p) = \frac{\bar{v}(p)}{\delta_e(p)} = \frac{-0.0001682(p+1.101)(p+6.351)(p-5.51)}{(p+0.519)(p+1.1)(p+0.0318)(p-0.0122)} \tag{59}$$

Slow transfer functions:

$$\overline{N_{Zs}}(s) = \frac{\overline{n_z}(s)}{\delta_e(s)} = \frac{-4.438(s+0.0000162)(s+0.281)}{(s-0.2088)(s+0.4898)} = \frac{-4.438(p+0.000001)(p+0.0172)}{(p-0.0128)(p+0.03)} \tag{60}$$

$$\bar{V}_s(s) = \frac{\bar{v}(s)}{\delta_e(s)} = \frac{-0.08135(s+36.75)}{(s-0.2088)(s+0.4898)} = \frac{-0.004987(p-2.253)}{(p-0.0128)(p+0.03)} \tag{61}$$

where $s = p/\epsilon$ represents the low-frequency scale.

Fast Transfer Functions:

$$\overline{N_{Zf}}(p) = \frac{\overline{n_z}(p)}{\delta_e(p)} = \frac{0.00194(p+39.6)(p-33.24)}{(p+1.1)(p+0.5247)} \tag{62}$$

$$\bar{V}_f(p) = \frac{\bar{v}(p)}{\delta_e(p)} = 0 \tag{63}$$

An interesting observation is that $\bar{v}$ is a pure slow variable because $\bar{V}_f(p) = 0$. This means that $\bar{V}(p)$ can be approximated by $\bar{V}_s(p/\epsilon)$. The Bode plots of $\bar{V}(p)$ and $\bar{V}_s(p/\epsilon)$ shown in Fig. 1 confirm this observation. The Bode plots of $\overline{N_Z}(p)$, $\overline{N_{Zf}}(p)$, and $\overline{N_{Zs}}(p/\epsilon)$ are given in Fig. 2. It can be easily verified that $\overline{N_{Zf}}(0) = \overline{N_{Zs}}(\infty) = 12.9$ dB, and that $\overline{N_Z}(p)$ is close to $\overline{N_{Zf}}(p) + \overline{N_{Zs}}(p/\epsilon) - \overline{N_{Zf}}(0)$. Finally, we have

Actuator:

$$A(p) = \frac{\delta_e(p)}{\delta_{ec}(p)} = \frac{536}{(p+20)(p+50)} \tag{64}$$

To satisfy the various flying qualities requirements stated in Ref. 12, the feedback control scheme of Ref. 12 is adopted. This scheme is shown in Fig. 4. The design problem now is to choose the constants K_n, K_u, and K_i and to design the compensator $C(p)$ to meet the following design specifications.

1) The short-period and phugoid mode damping ratios must be greater than 0.5.

2) The elevator loop-frequency response must satisfy the following: a) ± 10 dB gain margin and ± 45 deg phase margin; b) the loop gain crossover frequency must not exceed 3 rad/s; and c) the loop gain must lie within the low-frequency and the high-frequency gain boundaries shown in Fig. 3a.

To proceed with the sequential two-time-scale design procedure, we need to state design specifications for each of the slow and fast design problems. The damping ratio requirement 1 and the gain and phase margin requirement 2a are imposed on both designs. The crossover frequency requirement 2b is clearly a high-frequency requirement that is imposed on the fast design. As for the gain boundaries requirement 2c, the gain boundaries of Fig. 3a are decomposed into high-frequency and low-frequency gain boundaries as shown in Figs. 3b and 3c, respectively. The fast design needs to satisfy the gain boundary in Fig. 3b; the slow design needs to satisfy the gain boundary in Fig. 3c. Finally, the integrator constant K_i in the PI-controller $(p + K_i)/p$ is chosen to be of order $\mathcal{O}(\epsilon)$, i.e., $K_i = \epsilon\hat{K}_i$, where $\hat{K}_i$ is $\mathcal{O}(1)$, such that $(p + \epsilon\hat{K}_i)/p$ can be treated as a slow transfer function that is approximated in the high-frequency range by 1.

Fast Design

In the high-frequency range, the control scheme of Fig. 4 is simplified as follows: The purely slow transfer function $\bar{V}(p)$ is deleted since $\bar{V}_f(p)$ is zero. The $\overline{N_Z}(p)$ can be approximated by $\overline{N_{Zf}}(p)$. The actuator $A(p)$ is retained since it is a fast element. Then Fig. 4 reduces to Fig. 5. We denote $\overline{N_{Zf}}(p)A(p)$ in Fig. 5 by $G_f(p)$, which represents the fast model of the airplane and the augmented dynamics.

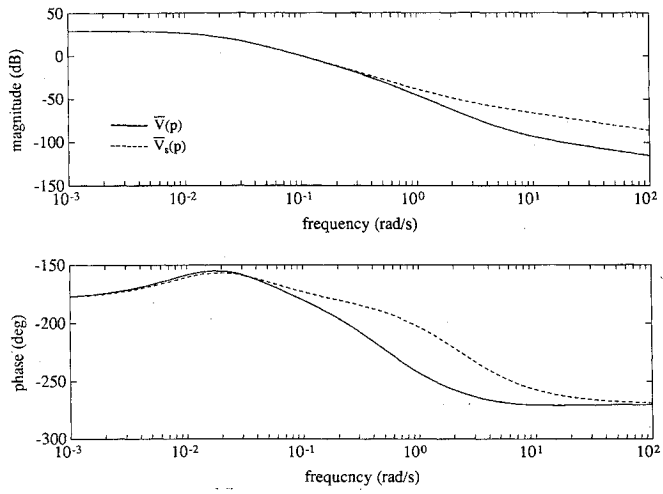

Fig. 1 Bode diagram of full incremental forward velocity $\bar{V}(p)$ and slow incremental forward velocity $\bar{V}_s(p)$.

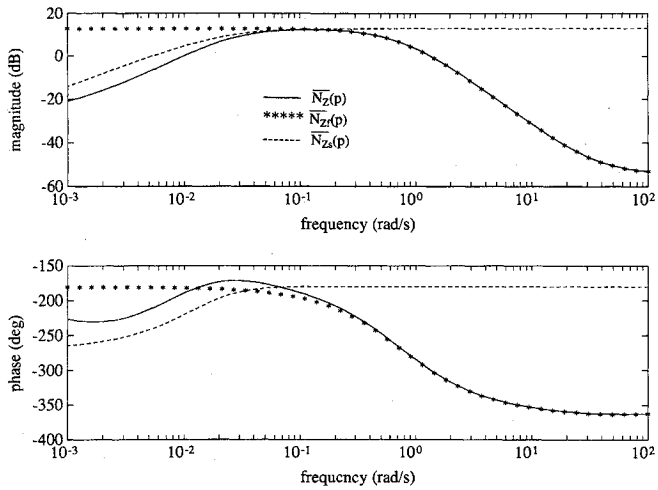

Fig. 2 Bode diagram of full normal acceleration $\bar{N}_Z(p)$, fast normal acceleration $\bar{N}_{Zf}(p)$, and slow normal acceleration $\bar{N}_{Zs}(p)$.

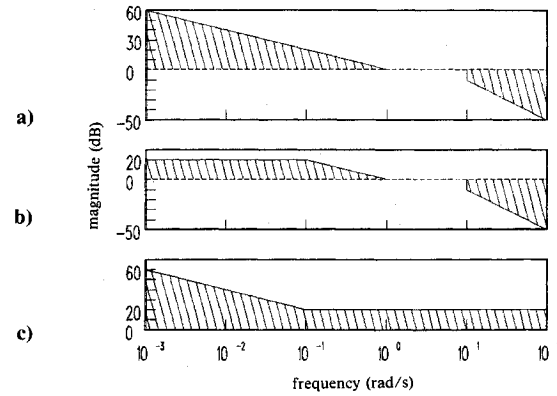

Fig. 3 Gain boundaries to be satisfied by a) the full design, b) the fast design, and c) the slow design.

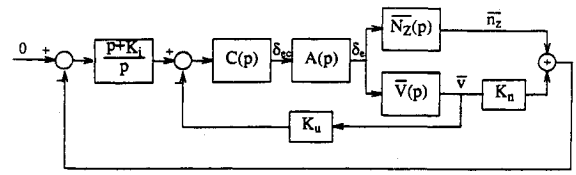

Fig. 4 Feedback control scheme for the full design.

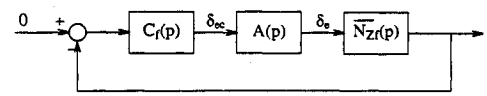

Fig. 5 Fast feedback control system.

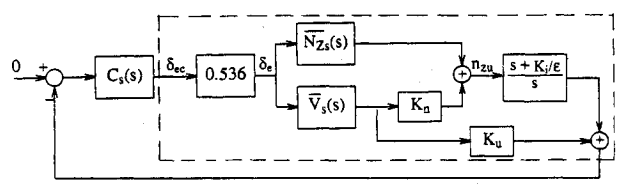

Fig. 6 Slow feedback control system.

Table 1 Summary of results from the fast, slow, and full designs

	Fast design	Slow design	Full design
Short-period mode	$\zeta=0.675$, $\omega_n=3.5$	—	$\zeta=0.693$, $\omega_n=3.13$
Phugoid mode	—	$\zeta=0.673$, $\omega_n=0.1$	$\zeta=0.681$, $\omega_n=0.082$
Gain margin	$\pm\infty$	-37 dB to ∞	-34 dB to ∞
Phase margin	-180 to 58 deg	-180 to 180 deg	-180 to 53 deg
Crossover frequency	2.33 rad/s	—	2.25 rad/s
Gain at 10 rad/s	-18.3 dB	—	-18.6 dB
Closed-loop poles (due to compensator)	-1.13, -1.65	-0.0736	-1.13, -1.88 -0.12
Closed-loop poles (due to actuator)	-21.3, -50.2	—	-21.2, -50.3

The design task is to find a fast compensator $C_f(p)$ that meets the design specifications for the fast design problem. It is important to note that the singular perturbation approximation is based on the assumption that the fast (high-frequency) dynamics and slow (low-frequency) dynamics are well separated, i.e., $\epsilon\to 0$. In the current case $\epsilon=0.0613$, which means that the short-period mode and the phugoid mode are only reasonably separated. Therefore, the design of $C_f(p)$ should be carefully done so that it would not disturb the separation between the slow and fast dynamics. Taking the frequency 0.1 rad/s as the intermediate point between the slow and fast dynamics, it is required that C_f satisfies the additional requirement $|G_f(0.1)C_f(0.1)-G_f(0)C_f(0)|<3$ dB. This requirement ensures that in the low-frequency range, the fast transfer function $G_f(p)C_f(p)$ can be approximated by its zero-frequency value.

The use of root locus and Bode plot techniques yield a lag-lead compensator

$$C_f(p)=\frac{-10.836(p+1.2)(p+1.2)}{(p+0.54)(P+6.8)} \tag{65}$$

which fulfills all design requirements, with $G_f(0)C_f(0)=20.07$ dB, and $G_f(0)C_f(0)-G_f(0.1)C_f(0.1)=2.5$ dB. Elevator loop Bode plots of the fast system are shown in Fig. 7. Other design results are summarized in Table 1.

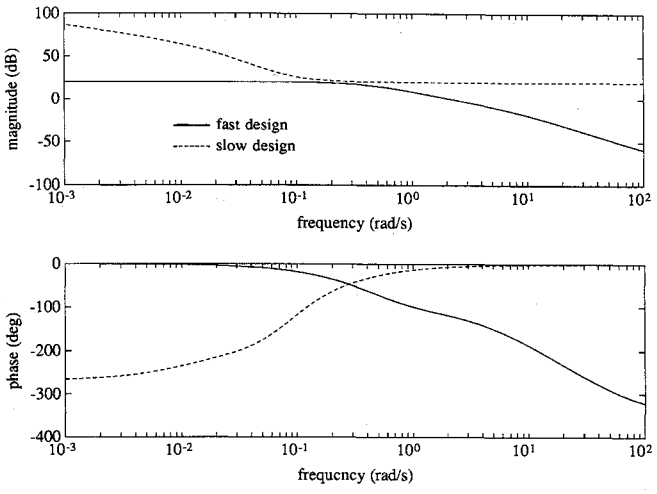

Fig. 7 Elevator open-loop frequency response of the fast design and the slow design.

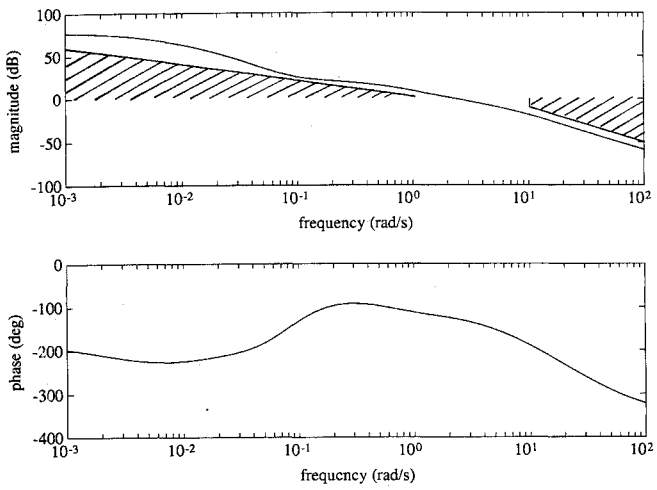

Fig. 8 Elevator open-loop frequency response of the full design.

Slow Design

In the low-frequency range, the control scheme of Fig. 4 can be modified as follows: $\overline{N_Z}(p)$ and $\overline{V}(p)$ are approximated by $\overline{N_{Zs}}(s)$ and $\overline{V}_s(s)$, respectively. The compensator $C(p)$ is replaced by $C_s(s)$. The PI-controller $(p+\epsilon\hat{K}_i)/p$ now becomes $(s+\hat{K}_i)/s$ in the low-frequency scale. The actuator $A(p)$ can be represented here by a constant

$$\left.\frac{536}{(\epsilon s+20)(\epsilon s+50)}\right|_{\epsilon=0}=0.536$$

since $A(p)$ is a fast element. For clarity, the slow control scheme is redrawn in Fig. 6, and the transfer function of the dashed box is denoted by $G_s(s)$, which represents the slow model of the airplane and the augmented dynamics.

The design task is to choose the constants K_n, K_u, and $\hat{K}_i$, and the slow compensator $C_s(s)$, to meet the slow design specifications. The constant K_n is taken as $K_n=-1.4889\ g^2$s/ft as specified in Ref. 12. The choice of the integrator constant $\hat{K}_i$ is a compromise between two factors. On one hand, $\hat{K}_i$ should not be too large because the corner frequency of $(s+\hat{K}_i)/s$ should lie in the low-frequency range (recall that the PI-controller has been approximated by 1 in the fast design). On the other hand, $\hat{K}_i$ should not be too small so that $(s+\hat{K}_i)/s$ can provide enough loop gain to meet the gain boundary requirement of Fig. 3c. As a compromise $\hat{K}_i$ is selected to be 3.6.

The design of the slow compensator $C_s(s)$ is subject to the constraint $C_s(\infty)=C_f(0)$, where $C_f(0)=-2.278$ is fixed in the fast design [see Eq. (65)]. As discussed in Sec. II, this constraint can be met by designing the strictly proper part $C_0(s)=C_s(s)-C_f(0)$ of $C_s(s)$ to stabilize the modified slow model

$$\hat{G}(s)=G_s(s)\left[I+C_f(0)G_s(s)\right]^{-1} \tag{66}$$

which is obtained by closing the loop around $G_s(s)$ with $C_f(0)$ in the feedback loop. The strict properness requirement should be interpreted to mean that $C_0(s)$ must roll off well before getting into the high-frequency range.

It is noticed during the design process that $C_f(0)=-2.278$ is large enough to introduce "high gain" effect into the slow design when the loop is closed around $\hat{G}_s(s)$ with $C_f(0)$ in the feedback loop. In other words, $C_f(0)$ is large enough to push the poles of $G_s(s)$ very close to the zeros of $G_s(s)$. The zeros of $G_s(s)$ depend on the constant K_u. When K_u is zero, $G_s(s)$ has a pair of lightly damped zeros at -0.1269 ± 0.9934, which can be moved to more stable locations by adjusting K_u. With the selection of $K_u=-6$, it turns out that the slow design requirements are satisfied with $C_0(s)=0$. Therefore, the slow compensator $C_s(s)$ is taken as

$$C_s(s)=C_0(s)+C_f(0)=C_f(0) \tag{67}$$

Elevator loop Bode plots of the slow system $[C_s(s),\ G_s(s)]$ are shown in Fig. 7. Other design results are summarized in Table 1.

Full Design

Once $C_f(p)$ and $C_0(s)$ have been designed [$C_0(s)$ is zero in this design example], the two-time-scale stabilizing compensator $C(p)$ of Fig. 4 can be taken as the parallel connection of $C_f(p)$ and $C_0(s)$, i.e.,

$$C(p)=C_0(p/\epsilon)+C_f(p)=\frac{-10.836(p+1.2)(p+1.2)}{(p+0.54)(p+6.8)} \tag{68}$$

Since the constants K_n, K_u, and $K_i=\epsilon\hat{K}_i$ have been selected, and the compensator $C(p)$ has been synthesized, we now have a solution for the full design problem. This full design is applied to the full system, as shown in Fig. 4, to check the design specifications. Elevator loop Bode plots are shown in Fig. 8. Other design results are summarized in Table 1. Comparison of the results of the full design with the corresponding results of the slow and fast designs shows that the performance of the full closed-loop system is indeed close to the performance of the slow and fast closed-loop systems. As a result of this closeness, the full design meets the design specifications, particularly as follows.

1) The short-period mode damping ratio is 0.693, and the phugoid mode damping ratio is 0.681. Both are larger than 0.5. It can be verified that the slow eigenvalues of the full design are $5.13\epsilon^2$ close to the eigenvalues of the slow design, and the fast eigenvalues of the full design are 6.11ϵ close to the eigenvalues of the fast design. These results comply with the claim about eigenvalue approximation in Sec. II. Since eigenvalues can be reasonably recovered in the full design, it is clear that damping ratios can be reasonably recovered as well.

2) Gain margin of the full design is -34 dB to ∞, covering the ±10 dB requirement. Phase margin of the full design is -180 to 53 deg, covering the ±45 deg requirement. Notice that the gain margin is determined by the slow design, whereas the phase margin is determined by the fast design (see Table 1).

3) The crossover frequency in the full design is 2.33 rad/s, which is close to the 2.25 rad/s of the fast design and less than 3 rad/s as required.

4) The elevator loop gain of the full system (Fig. 8) reasonably recovers the high-frequency loop gain of the fast design

(Fig. 7) and the low-frequency loop gain of the slow design (Fig. 7). It satisfies the gain boundaries requirement of 2c, stated previously. The results of specifications 2, 3, and 4 follow from the transfer function approximation result of Sec. II.

V. Conclusions

Longitudinal dynamics of an airplane can be modeled in the singularly perturbed form via scaling of state and output variables. This modeling step allows the singular perturbation approach to be applied to the control of longitudinal motion. In this paper, two results from singular perturbation theory are demonstrated. First, lower-order slow and fast models are obtained to represent the system at different frequencies. The accuracy of these models in approximating eigenvalues is demonstrated. Second, a sequential design procedure is used to design a two-time-scale compensator for an unstable transport airplane using the lower-order slow and fast models. The performance of the full closed-loop system under this compensator is shown to be reasonably close to the performance of the slow and fast closed-loop subsystems.

Acknowledgment

This work has been supported in part by the National Science Foundation under Grant ECS-8610714.

References

[1]Etkin, B., *Dynamics of Flight—Stability and Control,* Wiley, New York, 1982.

[2]McRuer, D., Ashkenas, I., and Graham, D., *Aircraft Dynamics and Automatic Control,* Princeton Univ. Press, Princeton, NJ, 1983.

[3]Gangsaas, D., Bruce, K. R., Blight, J. D., and Ly, U.-L., "Application of Modern Synthesis to Aircraft Control: Three Case Studies," *IEEE Transactions on Automatic Control,* Vol. AC-31, Nov. 1986, pp. 995-1014.

[4]Elliot, J. R., "NASA's Advanced Control Law Program for the F-8 Digital Fly-by-Wire Aircraft," *IEEE Transactions on Automatic Control,* Vol. AC-22, Oct. 1977, pp. 753-757.

[5]Sobel, K. M., and Shapiro, E. Y., "Application of Eigenstructure Assignment to Flight Control Design: Some Extensions," *Journal of Guidance, Control, and Dynamics,* Vol. 10, No. 1, 1987, pp. 73-81.

[6]Speyer, J. L., White, J. E., Douglas, R., and Hull, D. G., "Multi-Input/Multi-Output Controller Design for Longitudinal Decoupled Aircraft Motion," *Journal of Guidance, Control, and Dynamics,* Vol. 7, No. 6, 1984, pp. 695-702.

[7]Kokotovic, P. V., Khalil, H. K., and O'Reilly, J., *Singular Perturbation Methods in Control: Analysis and Design,* Academic, New York, 1986.

[8]Kokotovic, P. V., and Khalil, H. K., *Singular Perturbations in Systems and Control,* IEEE Press, New York, 1986.

[9]Khalil, H. K., "Output Feedback Control of Linear Two-Time-Scale Systems," *IEEE Transactions on Automatic Control,* Vol. AC-32, Sept. 1987, pp. 784-792.

[10]Luse, D. W., and Khalil, H. K., "Frequency Domain Results for Systems with Slow and Fast Dynamics," *IEEE Transactions on Automatic Control,* Vol. AC-30, Dec. 1985, pp. 1171-1179.

[11]Vidyasagar, M., *Control System Synthesis: A Factorization Approach,* MIT Press, Cambridge, MA, 1985.

[12]Blight, J. D., Gangsaas, D., and Richardson, T. M., "Control Law Synthesis for an Airplane with Relaxed Static Stability," *Journal of Guidance, Control, and Dynamics,* Vol. 9, No. 5, Sept. 1986, pp. 546-554.